

4-19-1982

## New neutron-rich $^{179}\text{Yb}$ and $^{181,182}\text{Lu}$ isotopes produced in reactions of 9 MeV $u^{136}\text{Xe}$ ions on tantalum and tungsten targets

R. Kirchner

*GSI Helmholtz Centre for Heavy Ion Research GmbH*

O. Klepper

*GSI Helmholtz Centre for Heavy Ion Research GmbH*

W. Kurcewicz

*GSI Helmholtz Centre for Heavy Ion Research GmbH*

E. Roeckl

*GSI Helmholtz Centre for Heavy Ion Research GmbH*

E. F. Zganjar

*GSI Helmholtz Centre for Heavy Ion Research GmbH*

*See next page for additional authors*

Follow this and additional works at: [https://digitalcommons.lsu.edu/physics\\_astronomy\\_pubs](https://digitalcommons.lsu.edu/physics_astronomy_pubs)

---

### Recommended Citation

Kirchner, R., Klepper, O., Kurcewicz, W., Roeckl, E., Zganjar, E., Runte, E., Schmidt-Ott, W., Tidemand-Petersson, P., Kaffrell, N., Peuser, P., & Rykaczewski, K. (1982). New neutron-rich  $^{179}\text{Yb}$  and  $^{181,182}\text{Lu}$  isotopes produced in reactions of 9 MeV  $u^{136}\text{Xe}$  ions on tantalum and tungsten targets. *Nuclear Physics, Section A*, 378 (3), 549-558. [https://doi.org/10.1016/0375-9474\(82\)90465-1](https://doi.org/10.1016/0375-9474(82)90465-1)

This Article is brought to you for free and open access by the Department of Physics & Astronomy at LSU Digital Commons. It has been accepted for inclusion in Faculty Publications by an authorized administrator of LSU Digital Commons. For more information, please contact [ir@lsu.edu](mailto:ir@lsu.edu).

---

**Authors**

R. Kirchner, O. Klepper, W. Kurcewicz, E. Roeckl, E. F. Zganjar, E. Runte, W. D. Schmidt-Ott, P. Tidemand-Petersson, N. Kaffrell, P. Peuser, and K. Rykaczewski

B



GSI 81-37  
C.

# GSI

GSI - 81 -37  
PREPRINT

CERN LIBRARIES, GENEVA



CM-P00069148

NEW NEUTRON-RICH  $^{179}\text{Yb}$  AND  $^{181,182}\text{Lu}$  ISOTOPES PRODUCED  
 IN REACTIONS OF 9MEV/u  $^{136}\text{Xe}$  IONS ON TANTALUM AND  
 TUNGSTEN TARGETS

R. KIRCHNER, O. KLEPPER, W. KURCEWICZ, E. ROECKL,  
 E.F. ZGANJAR, E. RUNTE, W.-D. SCHMIDT-OTT, P. TIDEMAND-  
 PETERSSON, N. KAFFRELL, P. PEUSER, K. RYKACZEWSKI

Submitted for Publication in Nuclear Physics A

OCTOBER 1981

Gesellschaft für Schwerionenforschung mbH  
 Planckstr. 1 · Postfach 110541 · D-6100 Darmstadt 11 · Germany

NEW NEUTRON-RICH  $^{179}\text{Yb}$  AND  $^{181},^{182}\text{Lu}$  ISOTOPES PRODUCED IN  
REACTIONS OF 9 MeV/u  $^{136}\text{Xe}$  IONS ON TANTALUM AND TUNGSTEN TARGETS

R. Kirchner, O. Klepper, W. Kurciewicz<sup>1</sup>, E. Roeckl, E.F. Zganjar<sup>2</sup>  
GSI Darmstadt, 6100 Darmstadt, Fed. Rep. of Germany

E. Runte, W.-D. Schmidt-Ott, P. Tidemand-Petersson  
II. Physikalisches Institut, Universität Göttingen  
3400 Göttingen, Fed. Rep. of Germany

N. Kaffrell, P. Peuser  
Institut für Kernchemie, Universität Mainz  
6500 Mainz, Fed. Rep. of Germany

K. Rykaczewski  
Institute of Experimental Physics, Warsaw University,  
00-681 Warsaw, Poland

Abstract: The new neutron-rich isotopes  $^{179}\text{Yb}$  and  $^{181},^{182}\text{Lu}$  were produced in multinucleon transfer reactions by irradiating  $\text{nat}_W/\text{Ta}$  targets with 9 MeV/u  $^{136}\text{Xe}$  ions, and identified by mass separation and decay spectroscopy. The measured half-lives of  $^{179}\text{Yb}$ ,  $^{181}\text{Lu}$  and  $^{182}\text{Lu}$  are  $8.1 \pm 0.8$ ,  $3.5 \pm 0.3$  and  $2.0 \pm 0.2$  min, respectively. The properties of the excited states of  $^{181},^{182}\text{Lu}$  are discussed. The possibility of studying neutron-rich nuclei outside the classical fission-product regions is demonstrated.

Darmstadt, October 1981  
(Submitted for publication in Nuclear Physics A)

<sup>1</sup> On leave of absence from Institute of Experimental Physics,  
University of Warsaw, 00-681 Warsaw, Poland

<sup>2</sup> On leave of absence from Department of Physics, Louisiana State  
University, Baton Rouge, Louisiana 70803, USA

E

RADIOACTIVITY  $^{179}\text{Yb}$ ,  $^{181},^{182}\text{Lu}$  (from  $\text{nat}_W/\text{Ta} + ^{136}\text{Xe}$ ,  
9 MeV/u, mass separation); measured  $E_\gamma$ ,  $I_\gamma$ ,  $\gamma\gamma$ -coinc,  $\gamma\beta$ -coinc,  
 $T_{1/2}$ ;  $^{179}\text{Lu}$ ,  $^{181},^{182}\text{Lu}$  deduced levels,  $I_\pi$ ,  $\pi$ , deduced  $\log ft$ .  
plastic scintillator and Ge(Li) detectors.

The integrated unit of target and thermal ion source<sup>5)</sup> used during these measurements is of particular interest, especially in view of the fact that its target thickness increases with running time.

The thermal ion-source cavity contains, stepping through in <sup>136</sup>Xe beam direction, three tungsten foils acting as windows and/or ionizing surface, and a tantalum foil (table 1). The latter foil is designed to act as a catcher in order to make use of the superior release properties of tantalum compared to tungsten for lanthanide elements<sup>6,7)</sup>. Due to the high temperature of the cavity - the window represents the "cold" spot at about 2500°C - the thicknesses of these foils vary dramatically with operation time because of evaporation and condensation of tantalum from the catcher foil, see table 1. If we consider the effective thickness<sup>9)</sup> of the tungsten/tantalum target to be about 20 mg/cm<sup>2</sup>, the original set of foils corresponds to approximately half of that effective layer being tungsten in which xenon-on-tungsten reactions occur at high projectile energies. The tantalum foil acts as a catcher for such reaction products with sufficiently high recoil energy and simultaneously as target and catcher for xenon-on-tantalum reaction products at energies < 6.6 MeV/u. With increasing operation time, however, reactions take place in a sandwich-type target of tungsten-tantalum layers which also gradually take over the role of the catcher. We therefore have to deal with a "thick tungsten/tantalum target" which is not well defined from the point of view of reaction kinematics, as well as with time variations of the overall on-line efficiency because the release efficiency depends on the catcher material<sup>6,7)</sup>.

3. Experimental results and discussion

The main aspect of the present study lies in the capability of producing new neutron-rich nuclei in the heavy-lanthanide region. The decay properties measured for the new ytterbium and lutetium isotopes are described in the following. The reaction yields for production of the neutron-rich lutetium isotopes are also presented.

3.1. THE <sup>179</sup>Yb → <sup>179</sup>Lu DECAY

Fig. 1 shows a part of the γ-ray spectrum measured for mass A=179. The lines assigned to the <sup>179</sup>Yb decay are labelled with energies. The time-

1. Introduction

With the availability of heavy-ion beams in the energy range up to 10 MeV/u and in the mass range from argon to uranium, such projectiles are used to study interactions with correspondingly heavy-mass targets. One motivation behind such studies is the possibility of reaching new neutron-rich isotopes by multinucleon transfer processes. This reaction path was first studied in the early work by Volkov et al. (see ref. 1). They were able to identify a series of hitherto unobserved isotopes of elements below argon using particle-identification techniques in an investigation of the reaction of 7.25 MeV/u <sup>40</sup>Ar ions with thorium targets. Even though this type of experiment has been continued, e.g. recently by Guerreaud et al.<sup>2)</sup> and Breuer et al.<sup>3)</sup>, it has almost exclusively been used for studying reaction kinematics and identifying new isotopes rather than for studies of their nuclear properties.

We have applied transfer reactions to produce neutron-rich isotopes of the lanthanide elements. In addition to previously known nuclides we identified the new isotopes <sup>179</sup>Yb, <sup>181</sup>Lu and <sup>182</sup>Lu. The intensities of mass-separated samples of these nuclides sufficed for decay-spectroscopic investigation, the results of which are presented.

2. Experimental techniques

The measurements were performed with a 9 MeV/u <sup>136</sup>Xe beam of 10 - 16 particle.nA intensity from the UNILAC accelerator at GSI, using the on-line mass separator<sup>4)</sup> for preparing sources whose β-, γ- and x-ray activities were investigated by singles (including multispectrum analysis) and coincidence measurements. For this purpose, two of the mass-separated beams were collected simultaneously at two movable-tape systems used to transport the activities into counting positions after preselected accumulation times. Each counting position was equipped with a 0.5 mm thick <sup>4</sup>π plastic scintillator and two Ge(Li) detectors in 180° geometry. For background reduction the γ-rays were gated by the signals from the plastic scintillators used as β-ray detectors.

analyses of  $\beta$ -rays (after correction for Lutetium  $\beta$ -rays) and the 612.5 keV  $\gamma$ -transition agreed within a half-life value of  $T_{1/2} = 8.1 \pm 0.8$  min. All the other transitions given in table 2 show a similar time dependence. A strong indication to assign these  $\gamma$ -lines to the  $\beta$ -decay of  $^{179}\text{Yb}$  is the coincidence with Lutetium KX-rays observed for the strongest transitions.

No information on levels of  $^{179}\text{Lu}$  was available prior to this study except for the configuration of the ground state ( $7/2^+$  [404]) which was deduced from the  $\beta$ -branching of  $^{179}\text{Lu}$  to  $^{179}\text{Hf}$  (ref. 10)). The coincidence information given in table 2 did not suffice to establish a level scheme of  $^{179}\text{Lu}$ . However, a level at 612.5 keV can tentatively be assigned on the basis of the strong intensity of this transition and its coincidence properties. A further level at 994.1 keV is suggested by the 994.2 keV transition and the 612-381 coincidence.

### 3.2. THE $^{181}\text{Lu} \rightarrow ^{181}\text{Hf}$ DECAY

The results of our singles and coincidence studies on the  $^{181}\text{Lu}$  decay are presented in table 3. In fig. 2 a part of the  $\gamma$ -ray spectrum of  $^{181}\text{Lu}$  is shown. The half-life of 3.5±0.3 min for  $^{181}\text{Lu}$  resulted from the analysis of the decay-curves of  $\beta$ -rays (see fig. 2), hafnium KX-rays and the  $\gamma$ -transitions with energies of 205.9 and 652.4 keV. A part of the level scheme of  $^{181}\text{Hf}$ , which is shown in fig. 3, was known already from (n, $\gamma$ ) and (d,p) reactions (10). In the present work, like from the reaction data (10), levels of the ground state rotational band built upon the  $1/2^-$  [510+] Nilsson configuration were deduced up to  $I^\pi = 7/2^-$ . The  $3/2^-$  [512+] state at 251.9 keV is in good agreement with the energy of 252 keV found in the study of the  $^{180}\text{Hf}$  (n, $\gamma$ ) reaction (10). Possible members of this rotational band are the states at 329.5 ( $5/2^-$ ) and 440.5 ( $7/2^-$ ) keV, compared with energies of 332 and 445 keV given in ref. (10). In addition, we have evidence for a level at 663.9 keV which might be identical with the  $7/2^-$  [503+] Nilsson state at 670 keV found in the (d,p) study (10).

A new level at 904.5 keV is established in the present work. Total transition intensities, shown in fig. 3, were determined from  $\gamma$ -ray intensity measurements and theoretical conversion coefficients (11). The  $\beta$ -branch of  $\sim 100\%$  to the 904.5 keV level was deduced from the intensity balance based on the assumption that the ground state of  $^{181}\text{Hf}$  is not directly fed in the  $\beta$ -decay of  $^{181}\text{Lu}$ . The log ft value of 4.7 for the

decay to the 904.5 keV level was determined using the "f $^\pi$ "-tables of ref. (12) and a  $Q_\beta$  value of 2.3 MeV. The current mass formulae (13) agree in predicting such a  $Q_\beta$  value within  $\pm 0.3$  MeV, which corresponds to a change of the log ft value of only -0.4. As the observed log ft value indicates, the corresponding  $\beta$ -transition should be of the allowed unhindered type.

From the systematics of Nilsson orbitals (10) the most probable ground-state configuration of  $^{181}\text{Lu}$  is  $7/2^+$  [404]. Spin and parity of  $5/2^+$  were assigned to the 904.5 keV state taking into account the selection rules for  $\beta$ -decay and the fact that this state decays by  $\gamma$ -transitions to  $3/2^-$ ,  $5/2^-$  and  $7/2^-$  states. The fast allowed  $\beta$ -transitions can occur in the considered mass region via the  $7/2^-$  [514],  $9/2^-$  [514] neutron-proton pair (14). Hence, the  $5/2^+$  state at 904.5 keV may be interpreted as a three-quasiparticle state with the configuration  $\pi 7/2^+$  [404],  $\nu 7/2^-$  [514],  $\pi 9/2^-$  [514]. A level at 1030.5 keV, decaying by the 590.0 keV  $\gamma$ -transition to the 440.5 keV state, might tentatively be introduced and interpreted as the first rotational  $7/2^+$  state of the  $K^\pi = 5/2^+$  band.

### 3.3 THE $^{182}\text{Lu} \rightarrow ^{182}\text{Hf}$ DECAY

Parts of the  $\gamma$ -spectrum measured for mass 182 are shown in fig. 4. The 97.8(2), 224.0(5), 720.8(5), 808.1(5) and 818.2(5) keV  $\gamma$ -transitions with relative intensities of 50(10), 15(7), 100(10), 50(15) and 100(25), respectively, were assigned to the  $^{182}\text{Lu}$  decay. The 97.8 and 224.0 keV transitions were previously known from the study of the 62 min  $^{182m}\text{Hf}$  decay (10). The  $^{182}\text{Lu}$  half-life of 2.0±0.2 min was obtained from the analysis of the decay-curves of  $\beta$ -rays (see fig. 4), hafnium KX-rays and the  $\gamma$ -transitions with energies of 97.8 and 720.8 keV. The final results led to the decay scheme presented in fig. 5. The  $\beta$ -feeding of the individual levels results from intensity balance under the assumption that the ground state of  $^{182}\text{Hf}$  is not directly fed in the  $\beta$ -decay of  $^{182}\text{Lu}$ . The log ft values given in fig. 5 were determined using a  $Q_\beta$  value of 4.1 MeV from mass predictions (ref. 13)) in the above-mentioned sense (see sec. 3.2). The new states at 818.4 and 906.0 keV, introduced on the basis of energy fits, might be interpreted as the  $2^+$  head of the  $\gamma$ -vibrational band and its first  $3^+$  rotational member, similar to those observed in  $^{184}\text{W}$  (ref. 10)), the isotope of  $^{182}\text{Hf}$ .

### 3.4 REACTION YIELDS

Assuming total intensities of 24% per  $\beta$ -decay for the 98.9 keV (fig. 3)

and 71% for the 97.8 keV transition (fig. 5), one can deduce saturation strengths (normalized to 10 particle·nA of  $^{136}\text{Xe}$ ) for the mass-separated  $^{181}\text{Lu}$  and  $^{182}\text{Lu}$  samples of 16.3 and 5.4 decays/s, respectively. If we assume furthermore, that these nuclei are produced from  $^{186}\text{W}$  (see fig.6) via three-proton-two-neutron and three-proton-one-neutron stripping reactions, respectively, and that the on-line overall efficiency is of the order of 10% (ref. 5), the measured source strengths correspond to production cross sections of 0.08 and 0.03 mb for  $^{181}\text{Lu}$  and  $^{182}\text{Lu}$ , respectively.

#### 4. Conclusion

To our knowledge this study of heavy ytterbium and lutetium isotopes represents the first successful attempt to use multinucleon transfer reactions with projectiles above iron for synthesizing new neutron-rich isotopes. The source strengths were high enough to allow  $\beta\gamma$ -spectroscopic investigations, including an interesting fast  $\beta$ -transition in the  $^{181}\text{Lu}$  decay. For the three new isotopes identified, satisfactory overall agreement between measured  $\beta$ -decay half-lives and predictions from the gross theory of  $\beta$ -decay (6) can be stated.

We conclude that multinucleon transfer reactions such as  $^{136}\text{Xe} + \text{tantalum/tungsten}$  can provide a powerful tool for studying neutron-rich isotopes in the heavy-lanthanide region. An extension towards more neutron-rich isotopes of ytterbium and lutetium seems to be possible, especially for the latter element, where the mass-separated beams are free of higher-Z reaction products which are not released from the ion source. First attempts to identify  $^{180}\text{Yb}$  and  $^{183}\text{Lu}$  were inconclusive, even though weak  $\beta$ -activities and, in the latter case, weak hafnium KX-rays were observed. In this context, this work has to be considered as a first step characterized by technical limitations on the target and projectile side. Concerning the power load on the ion source,  $^{136}\text{Xe}$  beam intensities of 30 particle·nA seem to be acceptable. Tentatively,  $^{136}\text{Xe}$  is attractive as projectile in view of its high N/Z ratio and its closed neutron-shell configuration which might lead to enhanced proton transfer.

One can imagine similar applications in other areas of the chart of nuclides outside the classical fission-product regions. The general advantage of covering the energy span between the high incident energy and the Coulomb barrier, thereby including both damped and quasi-elastic collisions, follows e.g. from the studies of the Xe + Au system by Kratz et al. (9,17).

It is interesting to note, that neutron pick-up contributions have not been observed unambiguously in the present study due to the special target situation, even though this effect which is of interest for producing isotopes with higher neutron excess cannot be completely excluded. More specific nuclear-structure effects in the reactions, for example those enhancing the neutron rich nucleon flow (8) ought to be taken into account in planning future experiments.

The authors would like to acknowledge the encouraging discussions with Profs. G. Herrmann and J. Żylicz, to thank K. H. Burkard, C. Bruske and W. Hüller for operating the separator and the UNILAC operating crew for delivering high-intensity  $^{136}\text{Xe}$  beams.

Table 1

Target-catcher thicknesses for the thermal ion-source and corresponding  $^{136}\text{Xe}$ -beam energies

Foil	Thickness (mg/cm <sup>2</sup> ) a)	$^{136}\text{Xe}$ beam energy (MeV/u) b)
outer tungsten window/ionizer	3.2 - 14.1	8.8 / 8.2 - 6.0
inner tungsten window	4.0 - 12.5	8.2 - 6.0 / 7.4 - 3.4
tungsten ionizer	3.9 - 7.5	7.4 - 3.4 / < 6.6
tantalum catcher	41.7 - 42.2 <sup>c)</sup>	< 6.6

a) The two values given for each foil correspond to the thicknesses measured before and after the 8 h operation period of the thermal ion source.

b) The numbers calculated are the entrance/exit energies of each foil, assuming the thickness given in the neighbouring column. The stopping power tables of Hubert et al.<sup>8)</sup> were used. The energy loss of about 0.2 MeV/u in the heat shields outside the ion source is included.

c) Separate measurements have shown evaporation of tantalum at a rate of  $\sim 3 \text{ mg/cm}^2 \text{ h}$ , which, however, is compensated by an approximately equal deposition rate of tungsten evaporated from the ion source body.

Table 2

Energies, intensities and coincidence relations for  $\gamma$ -rays following the decay of  $^{179}\text{Yb}$ .

energy <sup>a)</sup> (keV)	Relative intensity	Coincident $\gamma$ -lines (keV)
141.5(4)	6(2)	
147.3(3)	14(3)	324.6
324.6(4)	20(4)	147.3
351.6(3)	43(5)	141.5, 612.5
381.5(3)	26(3)	612.5
411.1(3)	17(4)	
426.5(6)	6(3)	
431.2(4)	8(4) <sup>-</sup>	
471.1(5)	6(3)	
500.1(4)	11(3)	
522.8(4)	12(6)	
612.5(3)	100(6)	351.6, 381.5
643.0(4)	11(3)	
653.6(3)	27(4)	
994.2(10)	4(2)	
1024.4(13)	7(3)	

a) Transitions with intensities higher than 14 relative units were assigned to the  $^{179}\text{Yb}$  decay by their coincidence with Lutetium KX-rays, the other  $\gamma$ -rays by half-life analyses.



FIGURE CAPTIONS

Fig. 1 Part of the  $\gamma$ -ray spectrum of  $^{179}\text{Yb}$  measured with a 30% Ge(Li) detector in  $\beta$ -coincidence. The unlabelled  $\gamma$ -rays could not be unambiguously assigned to the  $^{179}\text{Yb}$  decay. 11 tape-transport cycles were accumulated with 700 s collection, 0.2 s transport, and 700 s counting time each. The average  $^{136}\text{Xe}$  beam intensity was 11.3 particle $\cdot$ nA. The insert shows the decay of the 612.5 keV  $\gamma$ -rays measured in  $\beta$ -coincidence.

Fig. 2 High-energy part of the  $\gamma$ -ray spectrum of  $^{181}\text{Lu}$  measured with a 15% Ge(Li) detector in  $\beta$ -coincidence. 47 tape-transport cycles were accumulated with 350 s collection, 2 s transport and 350 s counting time each. The average  $^{136}\text{Xe}$ -beam intensity was 12.4 particle $\cdot$ nA. The insert shows the decay-curve of  $\beta$ -rays measured with a thin plastic scintillator.

Fig. 3 The decay scheme of  $^{181}\text{Lu}$ . Levels from  $^{180}\text{Hf}$  ( $n,\gamma$ ) and  $^{180}\text{Hf}$  ( $d,p$ ) reactions<sup>9)</sup> are given for comparison. Transitions which have been confirmed by the coincidence measurements are marked by dots; the other transitions have been placed on the basis of energy fits. The numbers given in parentheses are absolute transition intensities.

Fig. 4 Parts of the  $\gamma$ -ray spectrum of  $^{182}\text{Lu}$  measured with a 15% Ge(Li) detector in  $\beta$ -coincidence. 27 tape-transport cycles were accumulated with 350 s collection, 2 s transport and 350 s counting time each. The average  $^{136}\text{Xe}$ -beam intensity was 11.7 particle $\cdot$ nA. The insert shows the decay-curve of  $\beta$ -rays measured with a thin plastic scintillator.

Fig. 5 The decay scheme of  $^{182}\text{Lu}$ . Levels from the 62 min  $^{182\text{m}}\text{Hf}$  decay (ref.<sup>9)</sup>) are given for comparison (for comments cf. caption to fig. 3).

TABLE 3

Energies and intensities of  $\gamma$ -rays following the decay of  $^{181}\text{Lu}$

$\gamma$ -ray energy (keV)	Relative $\gamma$ -ray intensity <sup>a)</sup>	Assumed multi-polarity	$\gamma$ -ray energy (keV)	Relative $\gamma$ -ray intensity <sup>a)</sup>	Assumed multi-polarity
45.8(2)	30(5)	M1	329.0(5)	23(5)	E2
52.9(5)	18(4)	M1	334.4(5)	17(6)	E2
98.9(2)	16(6)	E2	341.7(5)	15(4)	E2
105.7(5)	18(3)	E2	463.5(7)	21(6)	E1
125.2(5)	15(3)	E2	574.8(5)	70(6)	E1
153.4(7)	12(5)	E2	590.0(10)	15(5)	E1
159.1(7)	7(3)	E2	652.4(7)	100(6)	E1
205.9(3)	73(6)	E2	700.4(8)	19(7)	E1
240.4(5)	21(6)	E1	806.0(8)	40(10)	E1
252.0(10)	8(4)	E2	858.5(8)	35(10)	E1

a) These values have to be multiplied by a factor of 0.326 to convert to absolute intensities per 100 disintegrations.

Fig. 6 A section of the chart of nuclides illustrating the studies of neutron-rich ytterbium and lutetium isotopes. The source strength values in atoms/s, given in parentheses for lutetium, ytterbium, thulium and erbium isotopes, are from a separate measurement with a 9.1 MeV/u 10 particle·na <sup>136</sup>Xe beam, a 3 mg/cm<sup>2</sup> thick tungsten window and a 30 mg/cm<sup>2</sup> thick tantalum target-catcher (15). Assuming an on-line overall efficiency of 10%, a source strength of 1400 atoms/s corresponds to a production cross section of 3.1mb.

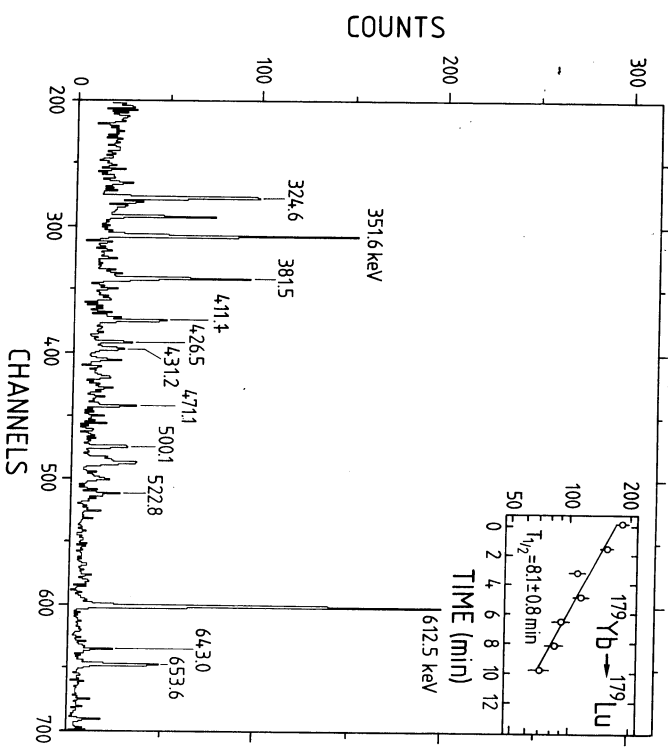


Fig. 1



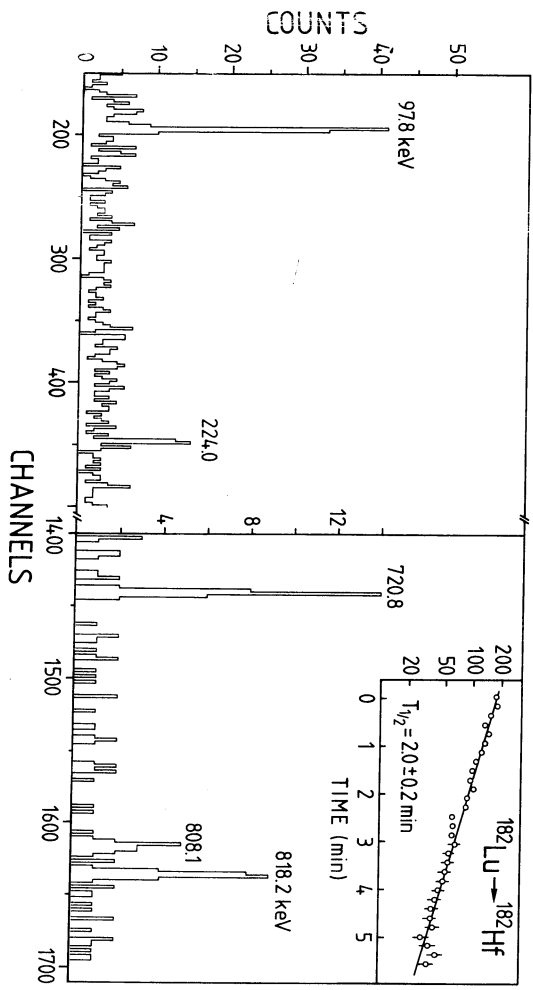


Fig. 4

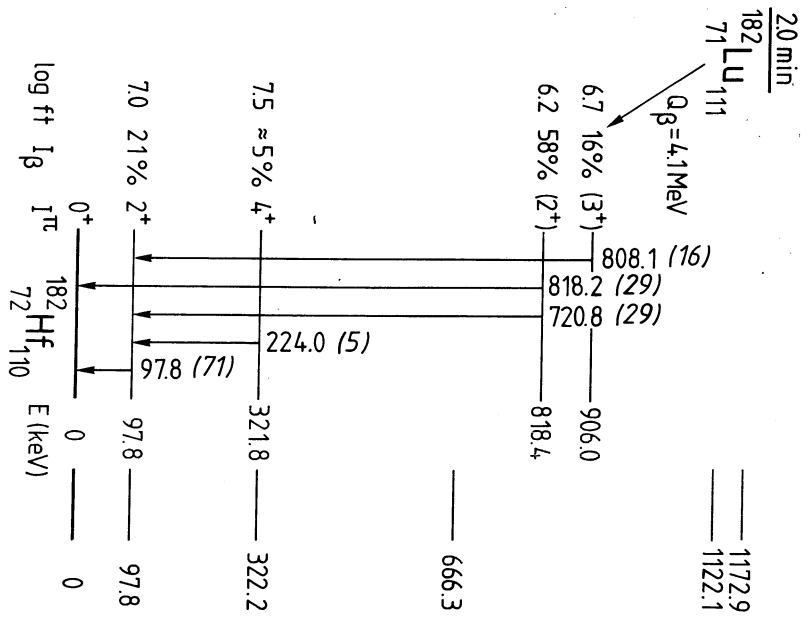


Fig. 5

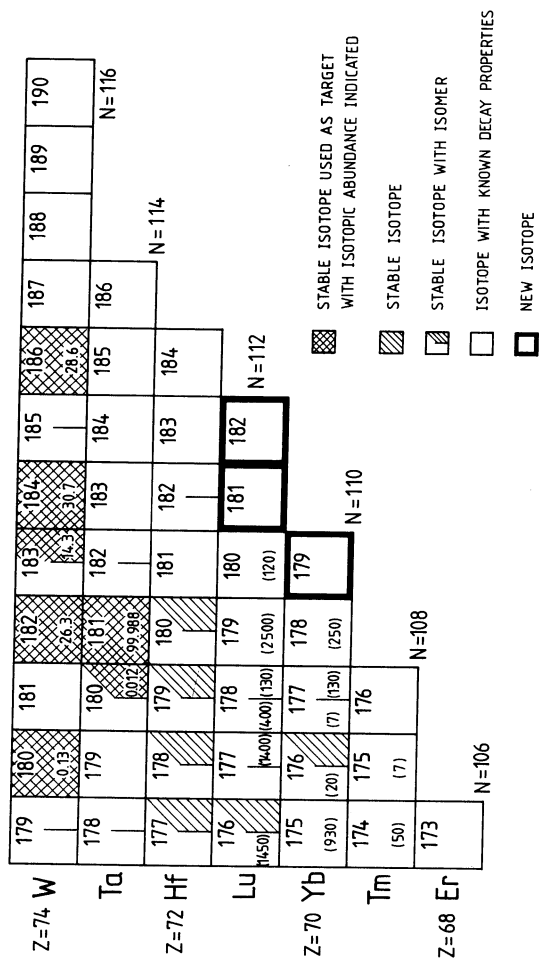


Fig. 6